

OAK RIDGE NATIONAL LABORATORY LIBRARIES



ORNL/TM-6560

3 4456 0551545 8

Nuclear Performance of Molten Salt Fusion-Fission Symbiotic Systems for Catalyzed DD and DT Reactors

M. M. H. Ragheb
R. T. Santoro
J. M. Barnes
M. J. Saltmarsh

OAK RIDGE NATIONAL LABORATORY

CENTRAL RESEARCH LIBRARY

CIRCULATION SECTION

4TH FLOOR ROOM 475

LIBRARY LOAN COPY

DO NOT TRANSFER TO ANOTHER PERSON

If you wish someone else to see this
report, send in name with report and
the library will arrange a loan.

U.S. GOVERNMENT PRINTING OFFICE: 1969 O 344-100

OAK RIDGE NATIONAL LABORATORY
OPERATED BY UNION CARBIDE CORPORATION - FOR THE DEPARTMENT OF ENERGY

10

11

12

ORNL/TM-6560
Distr. Category UC-20d
MFE-Fusion Systems

Contract No. W-7405-eng-26
Engineering Physics Division

NUCLEAR PERFORMANCE OF MOLTEN SALT FUSION-FISSION
SYMBIOTIC SYSTEMS FOR CATALYZED DD AND DT REACTORS*

M. M. H. Ragheb⁺
R. T. Santoro
J. M. Barnes**
M. J. Saltmarsh⁺⁺

* Submitted for
Journal publication

⁺ Present address:
Fusion Technology Program
University of Wisconsin
Madison, Wisconsin 53706

** Computer Sciences Division

⁺⁺ Fusion Energy Division

Date Published - March 1979

NOTICE This document contains information of a preliminary nature.
It is subject to revision or correction and therefore does not represent a
final report.

OAK RIDGE NATIONAL LABORATORY
Oak Ridge, Tennessee 37830
operated by
UNION CARBIDE CORPORATION
for the
DEPARTMENT OF ENERGY



3 4456 0551545 8

ACKNOWLEDGMENTS

Thanks are due to R. G. Alsmiller, Jr., R. W. Roussin, N. M. Greene, T. A. Gabriel, R. A. Lillie, W. E. Ford, III, W. W. Engle, J. E. White, M. A. Bjerke and Y. Seki for useful discussions. The manuscript preparation by Mrs. Coralee Zeigler is greatly appreciated.

NUCLEAR PERFORMANCE OF MOLTEN SALT FUSION-FISSION
SYMBIOTIC SYSTEMS FOR CATALYZED DD AND DT REACTORS

M. M. H. Ragheb , R. T. Santoro, J. M. Barnes and M. J. Saltmarsh
Oak Ridge National Laboratory, Oak Ridge, TN 37830

ABSTRACT

The nuclear performance of a fusion-fission hybrid reactor having a molten salt composed of Na-Th-F-Be as the blanket fertile material and operating with a catalyzed DD plasma is compared to a similar system utilizing a Li-Th-F-Be salt and operating with a DT plasma. The production of fissile fuel via the ^{232}Th - ^{233}U fuel cycle was considered on the basis of its potential nonproliferation aspects. The calculations were performed using one-dimensional discrete ordinates methods to compare neutron balances, fuel production rates, energy deposition rates, and the radiation damage in the reactor structure. The results indicate that the Na salt in conjunction with the catalyzed DD plasma represents a viable alternative to the Li salt and DT plasma. In a reactor consisting of a 42-cm thick salt compartment followed by a 40-cm thick graphite reflector, the Na-salt catalyzed-DD system exhibits a higher fissile nuclide production potential via $\text{Th}(n,\gamma)$ reactions (0.880 reactions/source neutron) than the Li salt-DT system (0.737 reactions/source neutron) without the additional complication of tritium production in the blanket. A 1000 MW(e) DD hybrid reactor is estimated to be able to support 14 fission reactors of the same power operating in the once-through cycle while a DT hybrid reactor can support about 8 fission reactors.

I. Introduction

A fusion-fission hybrid having a catalyzed DD plasma and a Na-Th-F-Be molten salt-filled blanket has been investigated as a fissile fuel source for fission reactors operating with the ^{232}Th - ^{233}U fuel cycle. The nuclear performance of the reactor is evaluated in terms of the neutron balance, fuel production rates, energy deposition rates, and the radiation damage to the first structural wall. These responses are also compared with those obtained for the same reactor configuration, but with a DT plasma and a blanket containing a Li-Th-F-Be salt as the fertile material. The calculational model of the reactor was based on the simple, compact Tokamak designs suggested by Steiner and his coworkers.¹⁻³ However, the general conclusions apply to both magnetic and inertial confinement systems.

The motivation for studying this concept was based on the potential for using a fusion-fission hybrid reactor as a fuel factory for fission reactors. This concept has been suggested as a possible near term application for fusion reactors.⁴⁻²⁰ In addition, the Pu/U cycle which has been used for fissile fuel production for Light Water Reactors, may represent safety and proliferation risks, so alternative fuel cycles are being considered. However, many of the alternative fuel cycles incorporate either nuclear poisons in various forms in the fuel or denaturing which results in economic penalties in fission reactors.^{4,5} The use of a neutron source such as a fusion reactor for breeding fissile fuel has, as a result, received considerable attention. The ^{232}Th - ^{233}U fuel cycle, as studied here, has been suggested as a possible nonproliferating fuel cycle alternative by Bethe⁶ and others.⁷⁻¹⁰

A fusion-fission hybrid reactor employing a catalyzed DD plasma is considered here for a variety of reasons. A catalyzed DD plasma eliminates the requirement for breeding tritium in the blanket. Consequently, the need for tritium storage, and its potential environmental hazard^{11,12} is eliminated. Also, the tritium produced in the DD cycle can be reinjected directly into the plasma, so the active tritium inventory in the plasma loop can be reduced by as much as a factor of three¹² compared to a DT system. Additionally, there is the advantage in the elimination of the competition for the neutrons to breed both tritium and fissile fuel that occurs in a DT system. Continuous extraction of the bred ^{233}U and its ^{233}Pa precursor would lead to a blanket relatively clean from fission product contamination and neutron poisoning and eliminate power swings caused by fissioning of the bred ^{233}U as occurs in solid blankets.

The reactor and blanket model, the plasma neutron sources, and details of the calculations are summarized in Sec. II. The results of the calculations are presented and discussed in Sec. III. The symbiosis of Light Water Reactors with the fusion-fission hybrid blanket is demonstrated in Sec. IV.

II. Reactor Configuration, Neutron Sources, and Details of the Calculations

The one-dimensional calculational model of the reactor blanket used in this study is summarized in Table I. The plasma cavity has a radius of 150 cm. The plasma neutron source is uniformly distributed in the central 100 cm radial zone and is isolated from the first structural wall by a 50-cm thick vacuum zone. The blanket module consists of a 1-cm thick stainless steel type 316 (SS-316) first structural wall cooled by a 0.5-cm thick water channel, a 42-cm thick molten salt-filled energy absorbing-breeding compartment, and a 40-cm thick graphite reflector. The molten salt and graphite are contained by 1-cm thick SS-316 structural shells.

Table I. Computational Model of the Reactor

Material	Zone	Outer Radius (cm)	Thickness (cm)	Remarks
Plasma	1	100.0	100	D-T (14.06 MeV) or catalyzed D-D (50% 2.45 MeV + 50% 14.06 MeV)
Void	2	150.0	50	Vacuum zone
First Wall	3	151.0	1.0	SS-316
Water	4	151.5	0.5	Cooling channel
Structure	5	152.5	1.0	
Molten Salt	6	194.5	42.0	NaF·BeF ₂ ·ThF ₄ or LiF·BeF ₂ ·ThF ₄ $\rho = 4.52 \text{ g/cm}^3$ (71-2-27 mole %)
Structure	7	195.5	1.0	
Graphite	8	235.5	40.0	Reflector
Structure	9	236.5	1.0	
Albedo*	10	-	-	-

* 20% albedo surface to simulate neutron and gamma ray reflection from a shield

Stainless steel was chosen as the first wall and structural material on the basis of known technology for the alloy in fusion reactor application.

The nuclear performance of the reactor was also assessed as a function of molten salt thickness, the volume fraction of SS-316 in the salt (to simulate additional structure and cooling tubes), and the thickness of the graphite reflector. Molten salt thicknesses of 21, 42, and 84 cm were

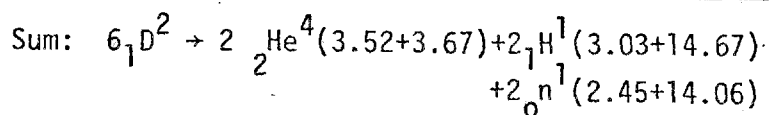
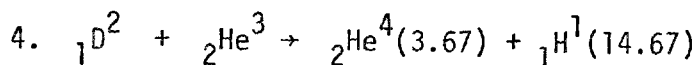
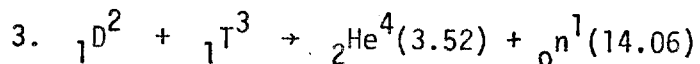
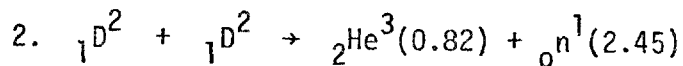
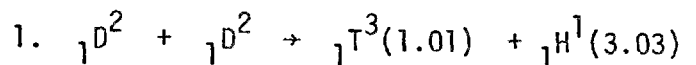
studied with the volume fraction of SS-316 in the salt ranging from 0 to 15% and for reflector thicknesses of 20 and 40 cm. A salt composed of Li-Th-F-Be was considered in conjunction with the DT plasma since the DT reaction must be fueled with tritium bred from neutron reactions with Li. A Na-Th-F-Be salt was used in the DD burning configuration since tritium breeding from neutron reactions with Li is not required. The compositions and nuclide densities of the materials used in the reactor model are summarized in Table II. The density of the two salts was kept constant as well as the mole fractions of the constituents (i.e., 71 m/o LiF-2 m/o BeF₂-27 m/o ThF₄ and 71 m/o NaF-2 m/o BeF₂-27 m/o ThF₄). The salt compositions are the same as those studied previously by Cook and Lidsky.⁵ For this analysis, only the blanket was included in the calculational model. The radiation reflected back into the blanket by the shield was accounted for by using a 20% albedo surface at the outer boundary of the blanket for all neutron and gamma ray energy groups.

The calculations were carried out using three plasma neutron sources: a catalyzed DD neutron source, a DT neutron source, and 2.45 MeV neutrons. The basic reactions occurring in the catalyzed DD plasma are shown in Table III. The numbers in parentheses are energies in MeV. (A detailed explanation of the catalysis process may be found in Ref. 21.) The plasma is predominantly a deuterium plasma. The first two reactions occur with almost equal probability and for these calculations it is assumed that they are equal. The catalysis is made to occur by adding just enough tritium and ³He to the plasma so that reactions (3) and (4) occur at the same rate as the DD reactions. By adding both sides it is noted that 6 deuterons are being converted into 2 helium atoms, 2 neutrons, and 2 protons.

Table II. Elemental Densities of Material Mixes

Material	Composition	Nuclides Density Nuclei/(barn·cm)
1 LiF-BeF ₂ -ThF ₄ Salt 71-2-27 Mole % ρ = 4.52 g/cm ³	⁶ Li	1.414-3
	⁷ Li	1.744-2
	Be	5.310-4
	Th	7.169-3
	F	4.859-2
2 NaF-BeF ₂ -ThF ₄ Salt 71-2-27 Mole % ρ = 4.52 g/cm ³	Na	1.697-2
	Be	4.779-4
	Th	6.452-3
	F	4.373-2
3 Stainless Steel 316 63.6 w/o Fe, 18 w/o Cr, 13 w/o Ni, 2.6 w/o Mo, 1.9 w/o Mn, 0.9 w/o (Si+Ti+C) ρ = 7.98 g/cm ³	C	1.990-4
	Si	1.360-3
	Ti	4.980-5
	Cr	1.150-2
	Mn	1.650-3
	Fe	5.430-2
	Ni	1.060-2
	Mo	1.290-3
4 Graphite, ρ = 2.25 g/cm ³	C	1.128-1
5 H ₂ O, ρ = 1 g/cm ³	H	6.687-2
	O	3.343-2

Table III. Catalyzed D-D Plasma Reactions



Reactions 1 and 2 are assumed equal.
 Reactions 3 and 4 proceed at the same rate
 as Reactions 1 and 2.

Steiner²² reported that for the DD cycle at an ion temperature of 400 keV, the fuel mixture consists of 88% D and 12% T. In this work, an energy distribution consisting of 50% 14.06 MeV neutrons (DT) and 50% 2.45 MeV neutrons (DD) was assumed. For the pure DT neutron source the energy distribution was taken to be 100% 14.06 MeV neutrons. Some data are also given for the case when the plasma is composed only of 2.45 MeV neutrons. The results obtained using this source, in combination with those obtained using the pure DT source, permit one to analyze the separate contributions to the various responses of the neutrons from the catalyzed DD neutron source or to estimate the responses for different neutron energy fractions.

Combining the results for different neutron source fractions is allowed because of the linearity of the radiation transport equation.

All of the calculations were performed using the one-dimensional discrete ordinates code ANISN²³ with a P_3 Legendre expansion, and an S_{12} angular quadrature. The transport cross sections were taken from the 100n-21 γ DLC 37 (ENDF/B-IV) library²⁴ and collapsed to a 35n-21 γ energy group subset. The energy group structure along with the fission spectrum in Th is shown in Table IV. All resonance nuclei were treated as being infinitely dilute. Cook and Maniscalco⁹ considered the effects of self-shielding in similar studies and observed only a 0.5% effect on their results, so omitting self-shielding in this work was not thought to seriously impact the results.

Energy deposition rates were estimated using neutron kerma factors generated from MACK²⁵ and MACKLIB²⁶ and using photon kerma factors generated with SMUG.²⁷ Radiation damage cross sections were calculated using the data base RECOIL²⁸, which generates atomic displacement and gas production cross sections in multigroup format from ENDF/B-IV point cross section data. All reaction cross section data were collapsed to the group structure shown in Table III using the COMAND module from AMPX.²⁷

It should be noted that the data for photon production in Th were not available in the ENDF/B-IV or the preliminary ENDF/B-V data files at the time this study was made. The heating rates obtained here for the molten salt zone are, as a result, somewhat underestimated.

It should also be noted that all of the calculated results are normalized to one source neutron so that renormalizing the results on the basis of reactor power or neutron wall loading can be easily carried out.

Table IV. Coupled 56 Neutron-Gamma Group Structure
and Fission Spectrum for ^{232}Th

Group	Neutron Lower Energy (eV)	Fission Spectrum	Group	Neutron Lower Energy (eV)	Fission Spectrum	Group	Gamma Lower Energy (eV)
1	1.3499+7*	5.3467-5	21	8.6517+4	1.5915-2	36	1.2+7
2	1.2214+7	1.3434-4	22	3.1828+4	1.0104-2	37	1.0+7
3	1.0000+7	9.3579-4	23	1.5034+4	2.0192-3	38	8.0+6
4	8.1873+6	3.3282-3	24	7.1018+3	6.6213-4	39	7.5+6
5	6.7032+6	8.9587-3	25	3.3546+3	2.1600-4	40	7.0+6
6	5.4881+6	1.9164-2	26	1.5846+3	7.0282-5	41	6.5+6
7	4.4933+6	3.3915-2	27	4.5400+2	2.8638-5	42	6.0+6
8	3.6788+6	5.1357-2	28	1.0130+2	4.6435-6	43	5.5+6
9	3.0119+6	6.8406-2	29	2.2603+1	4.8950-7	44	5.0+6
10	2.4660+6	8.1969-2	30	1.0677+1	3.8949-8	45	4.5+6
11	2.0190+6	9.0100-2	31	5.0435+0	1.2645-8	46	4.0+6
12	1.6530+6	9.2236-2	32	2.3824+0	4.1178-9	47	3.5+6
13	1.3534+6	8.9046-2	33	1.1254+0	1.3204-9	48	3.0+6
14	1.1080+6	8.2002-2	34	4.1400-1	4.9779-10	49	2.5+6
15	9.0718+5	7.2542-2	35	1.0000-4	1.4295-10	50	2.0+6
16	7.4274+5	6.2179-2				51	1.5+6
17	4.9787+5	9.4306-2				52	1.0+6
18	3.3373+5	6.0947-2				53	4.0+5
19	2.2371+5	3.7327-2				54	2.0+5
20	1.4996+5	2.2052-2				55	1.0+5
						56	1.0+4

*Read as $1.3499+7 = 1.3499 \times 10^7$

Upper energy of first neutron group is $1.4918+7$

Upper energy of first gamma group is $1.4000+7$

III. Discussion of Results

A. Neutron Balances

The equation

$$S + R(\nu\sigma_f) + R(\sigma_{n,2n}) + 2R(\sigma_{n,3n}) = L + R(\sigma_a) \quad (1)$$

defines the neutron sources and sinks in the reactor. In the equation

S is unit neutron source,

$R(\sigma)$ is a given reaction rate, $N\sigma\phi$, per source neutron,

(ϕ is the scalar flux, N is the nuclide density, and σ is the microscopic cross section)

L is the leakage rate per source neutron from the system, and

$$\sigma_a = \sigma_\gamma + \sigma_{\text{disappearance}}$$

$$\sigma_{\text{disappearance}} = \sigma_{n,p} + \sigma_{n,\alpha} + \sigma_{n,t} + \dots$$

The $\sigma_{\text{disappearance}}$ cross section takes into account all of the reactions in which the neutron disappears except for $(n,2n)$ and $(n,3n)$ reactions.

The convention is the same as that used with multigroup processed cross sections. The factor of two multiplying the $R(\sigma_{n,3n})$ reaction rate arises since one neutron is lost in the reaction while two are gained.

Tables V and VI show the neutron balances in the reactors using the catalyzed DD plasma with the Na salt and the DT plasma with the Li salt, respectively. These data were obtained for the reactor configuration with a 42-cm thick molten salt region, a 40-cm thick graphite reflector, and no stainless steel structure in the salt region. The neutron production rates are given as a function of the various material zones in the reactor. (See Table I)

The total neutron production rate is larger in the DT system than in the DD system because of the larger proportion of 14-MeV neutrons. This also leads to the slightly higher neutron leakage rate. The neutron

Table V. Neutron Balance in the Reactor with the Catalyzed DD Plasma

Zone Reaction	1	3	4	5	6	7	8	9	Total
Source	1.00+0*								1.00+0
Th($\nu\sigma_f$)					6.60-2				6.60-2
Th(n,2n)					5.23-2				5.23-2
2xTh(n,3n)					2.95-2				2.95-2
⁶ Li(n,2n)									
⁷ Li(n,2n)									
Ni(n,2n)		1.17-3		8.30-4		5.76-6		5.92-8	2.01-3
Cr(n,2n)		3.26-3		2.32-3		1.60-5		1.67-7	5.60-3
⁹ Be(n,2n)					1.88-3				1.88-3
Fe(n,2n)		1.90-2		1.35-2		8.93-5		8.66-7	
Mn(n,2n)		1.02-3		7.28-4		5.42-6		5.96-8	1.75-3
Na(n,2n)					1.59-4				1.59-4
Ti(n,2n)		1.90-5		1.34-5		9.02-8		8.83-10	3.25-5
Si(n,2n)		5.15-5		3.70-5		2.82-7		3.21-9	8.88-5
F(n,2n)					8.99-3				8.99-3
Mo(n,2n)		1.60-3		1.17-3		1.03-5		1.35-7	2.78-3
Total neutron production	1.00+0	2.61-2		1.86-2	1.59-1	1.27-4		1.29-6	1.20+0
Neutron absorption		1.01-1	5.23-3	8.47-2	9.89-1	1.19-2	2.28-3	3.72-3	1.19+0
System leakage									6.46-3

* Read as 1.00+0 = 1.00 x 10⁰

Salt composition: NaF-BeF₂-ThF₄

Salt region thickness: 42 cm

Reflector thickness: 40 cm

No SS-316 structure in the salt region

Table VI. Neutron Balance in the Reactor with the DT Plasma

Zone Reaction	1	3	4	5	6	7	8	9	Total
Source	1.00+0*								1.00+0
Th($\nu\sigma_f$)					1.24-1				1.24-1
Th(n,2n)					1.18-1				1.18-1
2xTh(n,3n)					6.06-2				6.06-2
$^6\text{Li}(n,2n)$					8.80-4				8.80-4
$^7\text{Li}(n,2n)$					8.06-3				8.06-3
Ni(n,2n)		2.33-3		1.66-3		8.20-6		8.28-8	4.00-3
Cr(n,2n)		6.52-3		4.63-3		2.30-5		2.38-7	1.12-2
$^9\text{Be}(n,2n)$					4.07-3				4.07-3
Fe(n,2n)		3.80-2		2.69-2		1.24-4		1.18-6	6.50-2
Mn(n,2n)		2.03-3		1.45-3		8.00-6		8.54-8	3.49-3
Na(n,2n)									
Ti(n,2n)		3.79-5		2.68-5		1.25-7		1.21-9	6.48-5
Si(n,2n)		1.03-4		7.41-5		4.23-7		4.69-9	1.78-4
F(n,2n)					1.86-2				1.86-2
Mo(n,2n)		3.21-3		2.36-3		1.66-5		2.08-7	5.59-3
Total neutron production	1.00+0	5.22-2	-	3.71-2	3.34-1	1.80-4	-	1.80-6	1.42+0
Neutron absorption	-	9.91-2	6.76-3	7.60-2	1.21+0	1.05-2	3.04-3	4.48-3	1.41+0
System leakage									7.98-3

* Read as 1.00+0 = 1.00×10^0

Salt composition: LiF-BeF₂-ThF₄

Salt region thickness: 42 cm

Reflector thickness: 40 cm

No SS-316 structure in the salt region

multiplication rate is also greater in the SS-316 first structural wall with most of the contribution arising from neutron reactions with Fe followed by a lesser contribution from reactions with Cr. In both reactor configurations, the largest fraction of the neutron multiplication comes from the $\text{Th}(\nu\sigma_f)$ and $\text{Th}(n,2n)$ reactions followed by the $\text{Th}(n,3n)$ and $\text{F}(n,2n)$ reactions. The contributions from the $\text{Na}(n,2n)$ reaction in the DD system and the ${}^6\text{Li}(n,2n)$ and ${}^7\text{Li}(n,2n)$ reactions in the DT system are small.

It is interesting to note that the neutron multiplication from fluorine is much larger than that from beryllium in both configurations. Since the neutron multiplication from beryllium is so small it would be to some advantage to consider salts which do not contain Be (which is scarce) in the DD system. Moreover, beryllium transmutes to ${}^6\text{He}$ via the (n,α) reaction which in turn decays to ${}^6\text{Li}$ via beta decay with a 805 msec half life. Slow neutron reactions with ${}^6\text{Li}$ will in turn produce tritium which can contaminate the salt therefore requiring additional chemical plant facilities for separating the isotope.

The total neutron multiplication is 1.2 for the DD system and 1.4 for the DT system with the $\text{Th}(\nu\sigma_f)$ reaction contributing 0.066 and 0.124 to each system, respectively. This implies less fission product contamination in the DD system than in the DT system. However, this is offset by the activated ${}^{24}\text{Na}$ isotope in the Na salt. The $\text{Th}(n,2n)$ reaction contributes almost as much to the neutron multiplication as fission (0.052 for the DD system and 0.118 for the DT system) followed by the $\text{Th}(n,3n)$ reaction (0.029 for the DD system and 0.061 for the DT system).

The spatial distributions of the major neutron multiplying reactions are shown in Fig. 1. As expected, the multiplication rate is larger in the DT system and in both cases the multiplication follows essentially the same exponential decay as the high energy neutron flux.

A series of calculations were performed to define an optimum thickness of the molten salt compartment and graphite reflector as a function of the neutron and secondary gamma ray leakage rate. The leakage rate as a function of the reflector thickness for a 42-cm thick molten salt compartment is shown in Fig. 2a. The neutron leakage rate is reduced by an order of magnitude when the reflector thickness is increased from 20 to 40 cm. The gamma ray leakage rate decreases by approximately a factor of eight. The leakage rate as a function of the thickness of the molten salt compartment is shown in Fig. 2b. These data were obtained using a 40-cm thick reflector in the calculational model. Increasing the molten salt compartment thickness results in an appreciable decrease in the leakage rate. In the remainder of this study, a molten salt thickness of 42 cm in combination with a 40-cm thick reflector was selected for the calculational model. Using a thinner salt or reflector results in a large leakage rate with resulting neutron economy problems particularly with respect to fissile and fusile breeding. On the other hand, an 84-cm thick salt compartment does not provide sufficient reduction in the leakage to merit the adoption of a very thick blanket.

B. Fissile and Fusile Fuel Breeding

The spatial dependences of the fissile and fusile fuel breeding rates as a function of depth in the molten salt compartment in the DD and DT reactors are shown in Fig. 3. The dependences of the $\text{Th}(n,\gamma)$, ${}^6\text{Li}(n,\alpha)$,

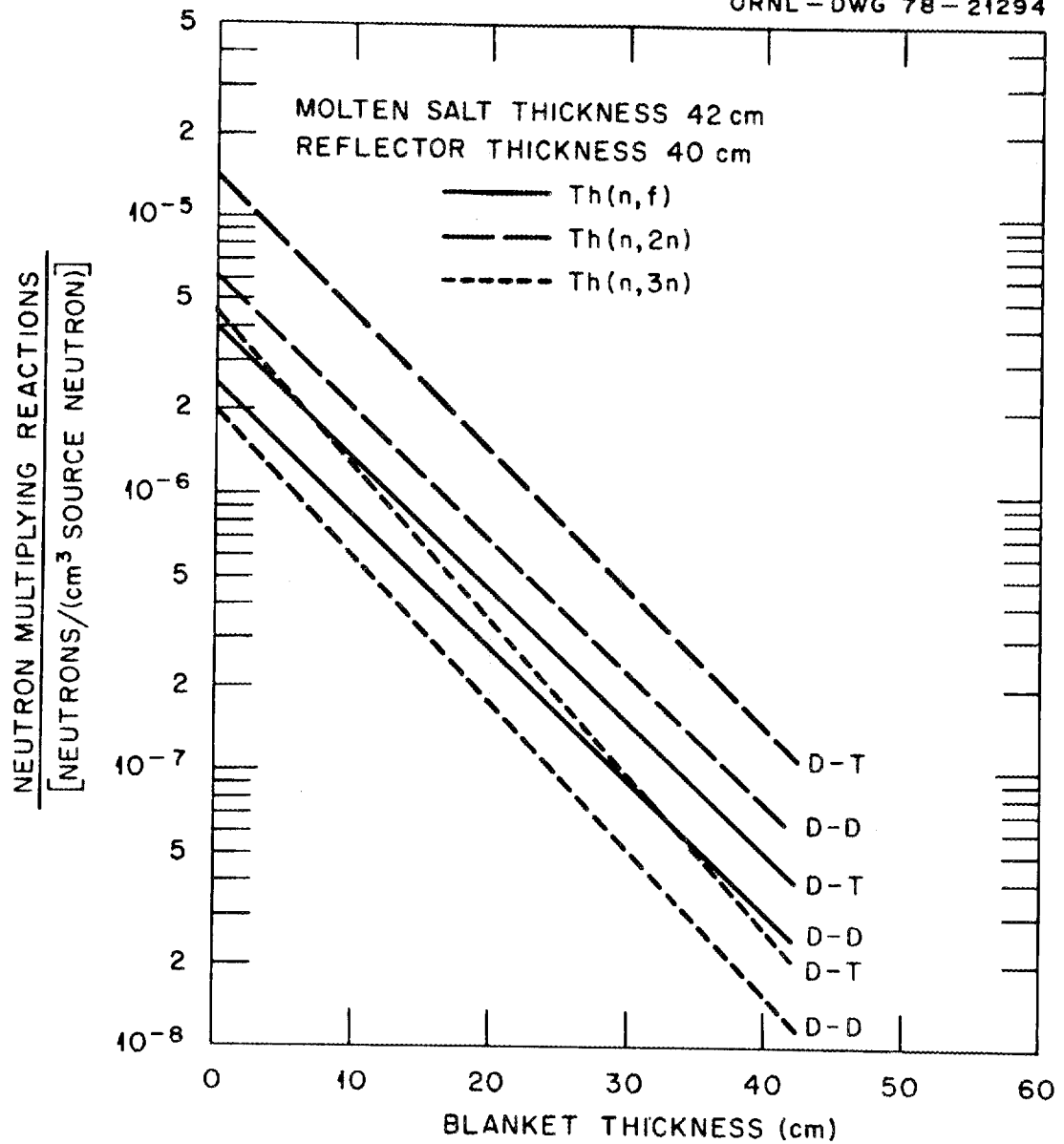


Fig. 1. Spatial distribution of the major neutron multiplying reactions for the DD and DT systems.

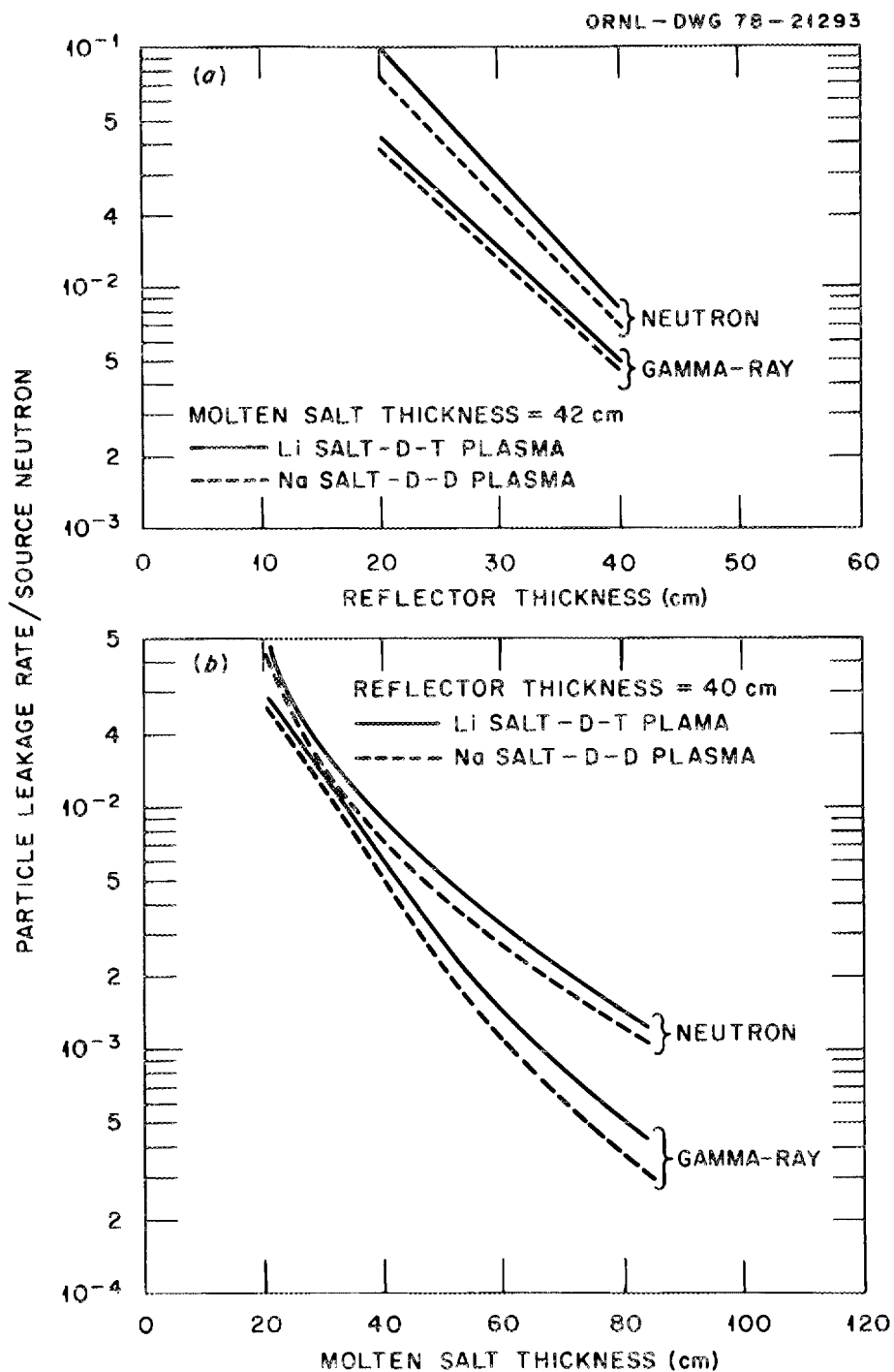


Fig. 2. Leakage rates for different reflector and molten salt compartment thicknesses.

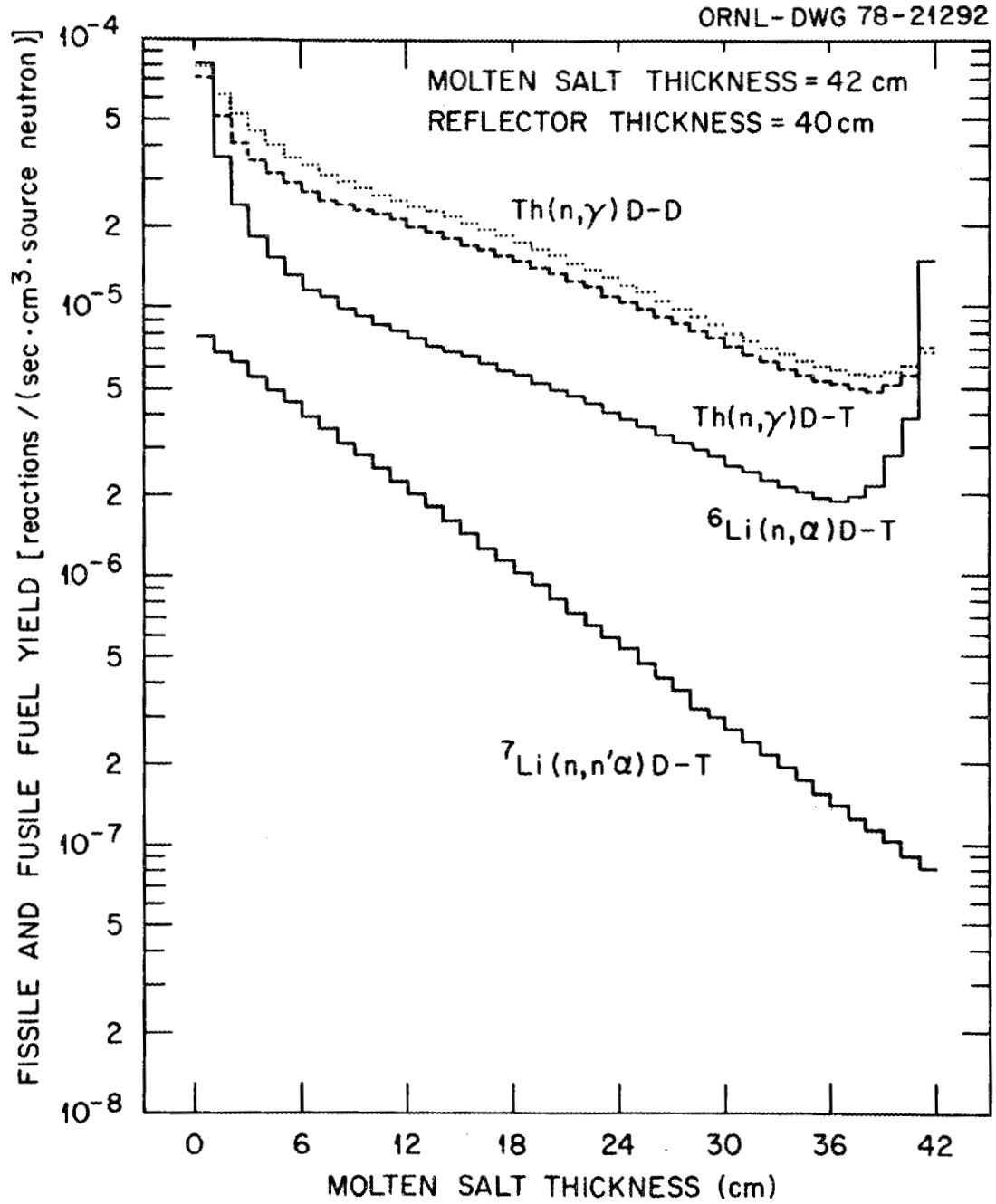


Fig. 3. Spatial dependences of fissile and fusile breeding in the molten salt compartment for the DD and DT systems.

and ${}^7\text{Li}(n,n'\alpha)$ reactions are shown for the DT system and the $\text{Th}(n,\gamma)$ reaction is shown for the DD system. The $\text{Th}(n,\gamma)$ reaction rate is higher in the DD reactor blanket than in the DD blanket. This is due, in part, to the competition for neutrons that takes place between the $\text{Th}(n,\gamma)$ and ${}^6\text{Li}(n,\alpha)$ reactions. They occur to a great extent as the result of slow neutron interactions and, therefore, compete with each other. Eliminating the requirement for tritium breeding in the DD reactor blanket results in the added advantage of a higher $\text{Th}(n,\gamma)$ reaction rate.

A quantitative comparison of the fusile and fissile breeding characteristics of the DD and DT systems are shown in Table VII. The breeding rates in both salt compositions are given for the three neutron sources described above. Since the radiation transport is linear, the fuel production rates may be obtained for any neutron source proportion introduced by different plasma ion temperatures by linearly interpolating among the 2.45 MeV and 14.06 MeV neutron sources.

The largest $\text{Th}(n,\gamma)$ reaction rate (0.996) occurs when the Na salt is used in conjunction with the DT reaction. For this case, however, the tritium required to fuel the plasma must be supplied to the system since that produced in the blanket is negligible. A system of this kind has been proposed and studied by Blinken and Novkov.^{19,20} For the catalyzed DD plasma, the $\text{Th}(n,\gamma)$ reaction rate is 0.880 in the Na salt compared to 0.737 obtained in the DT system using the Li salt. Also, for the DT system, the tritium breeding rate is 0.467 tritium nuclei per source neutron. The tritium production rate is too low to sustain the DT plasma and an external supply of the isotope is required to supplement the plasma. Thermal fission reactors can produce the required tritium either

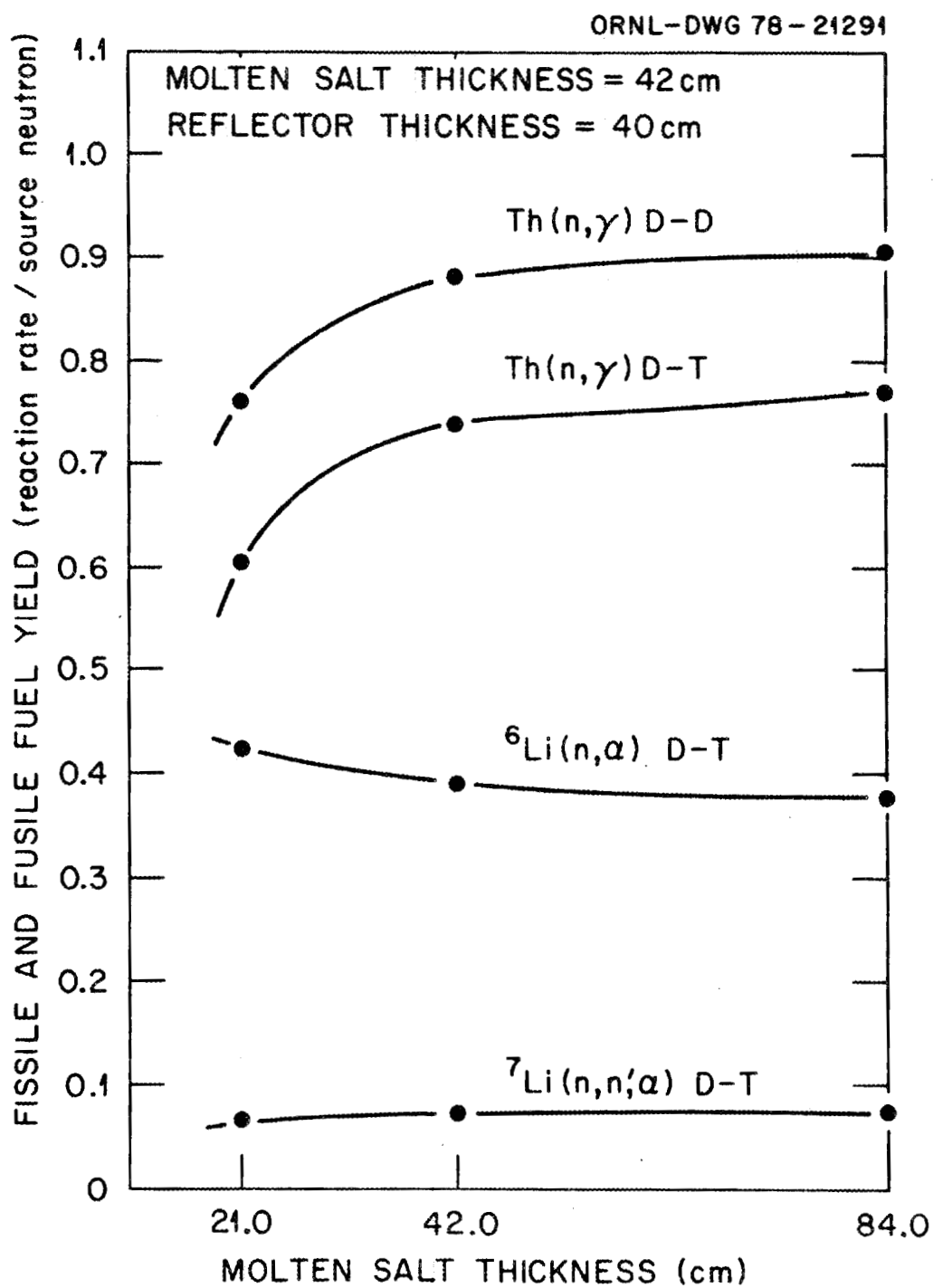


Fig. 4. Fusile and fissile breeding as a function of the molten salt region thickness for the DT and DD systems.

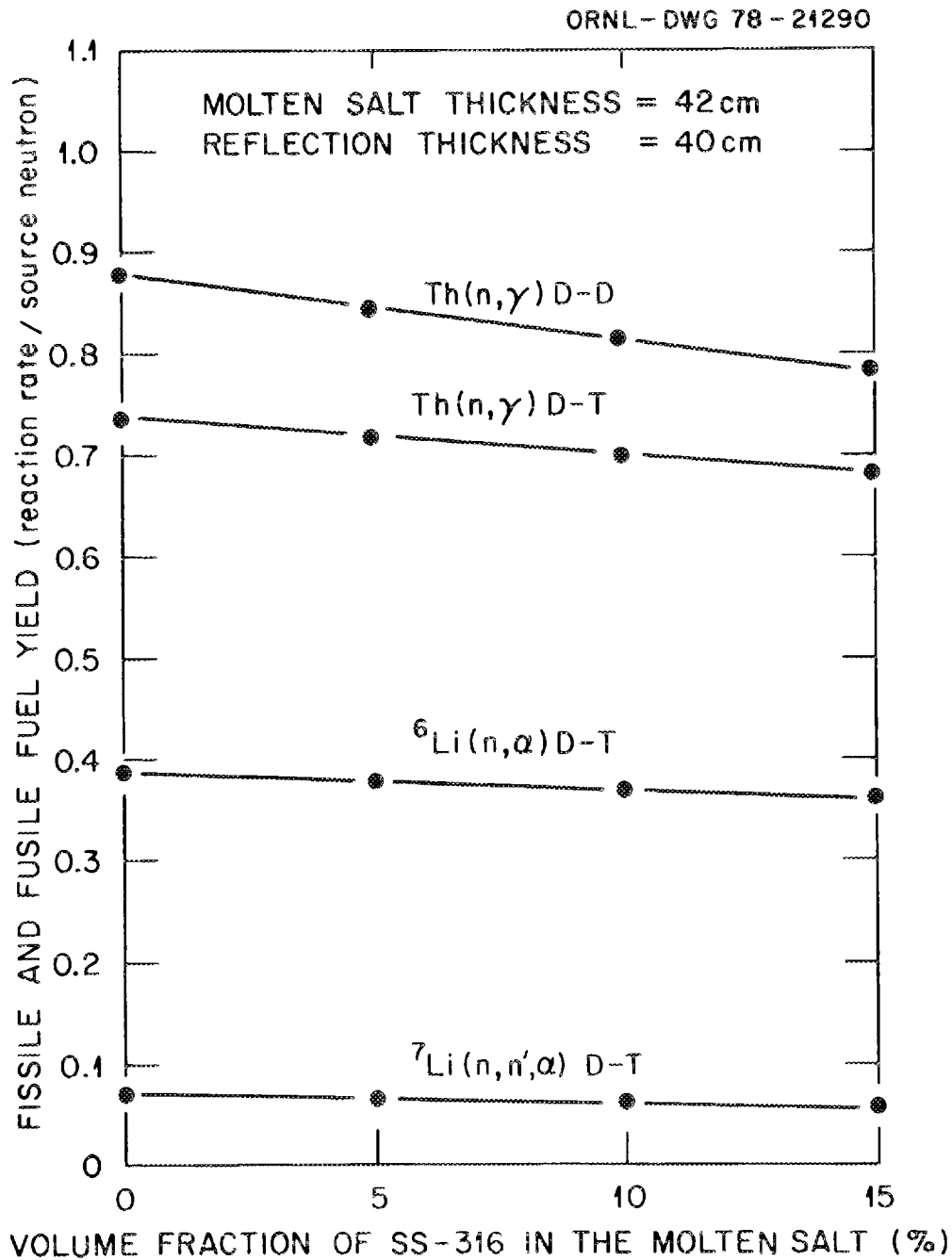


Fig. 5. Fissile and fusile production as a function of the amount of stainless steel structure present in the molten salt region for the DT and DD systems.

Table VII . Comparison of the Fissile and Fusile Breeding Characteristics for Li and Na Salts in DT and DD Symbiotic Fusion-Fuel-Factories

Source	Li-Be-Th-F Salt						Na-Be-Th-F Salt			
	${}^6\text{Li}(n,\alpha)\text{T}$	${}^7\text{Li}(n,n'\alpha)$	${}^9\text{Be}(n,\text{T})$	F(n,T)	Total T	Th(n, γ)	${}^9\text{Be}(n,\text{T})$	F(n,T)	Total T	Th(n, γ)
	(Nuclei/Source Neutron)									
100% 2.45 MeV	0.311	0.001	4.03-10	1.01-7	0.312	0.579	4.18-10	1.04-7	1.04-7	0.794
100% 14.06 MeV DT	0.391	0.073	1.08-4	3.33-3	0.467	0.737	1.04-4	3.08-3	3.18-3	0.966
50% 2.45 MeV +50% 14.06 MeV Catalyzed DD	0.351	0.037	5.40-5	1.67-3	0.390	0.658	5.20-5	1.54-3	1.59-3	0.880

Blanket thickness: 42 cm
 Reflector thickness: 40 cm
 No structure in salt region

on a dedicated basis or as a by-product. The fissile fuel production rate is higher in the DD system because of the absence of lithium in the salt which introduces the competition for neutrons between the ${}^6\text{Li}(n,\alpha)$ and $\text{Th}(n,\gamma)$ reactions.

Figure 4 shows the fusile and fissile breeding rates as a function of the molten salt region thickness for the DT and DD systems. In both configurations, $\text{Th}(n,\gamma)$ reactions tend to saturate at molten salt thickness ≈ 40 cm and since little extra fissile breeding is gained for thicker blankets, a blanket having a 42-cm thick breeding compartment was selected for this study. In the DT system, the ${}^6\text{Li}(n,\alpha)\text{T}$ and $\text{Th}(n,\gamma)$ reactions are competing. The $\text{Th}(n,\gamma)$ reaction rate increases with molten salt region thickness while the ${}^6\text{Li}(n,\alpha)\text{T}$ reaction rate decreases, but their sum is almost constant. The absence of the ${}^6\text{Li}(n,\alpha)\text{T}$ reaction in the Na salt with the catalyzed DD source leads to higher $\text{Th}(n,\gamma)$ reaction rates than in the DT case, inspite of the lower energy of DD neutrons.

The effect on the breeding due to the inclusion of stainless steel structure in the molten salt compartment in the catalyzed DD and DT systems is shown in Fig. 5. Structural material volume percentages in the molten salt of 5, 10, and 15% were considered. The fusile and fissile breeding rates decrease linearly with the addition of structural material to the salt. The $\text{Th}(n,\gamma)$ reaction rate in the catalyzed DD system is most sensitive to the amount of structure in the molten salt compartment.

C. Energy Deposition Rates

The volume-integrated neutron, gamma ray, and total (neutron plus gamma ray) energy deposition rates in the blanket, as well as the fractional total energy deposition rates, are summarized in Table VIII for the

Table VIII. Volume-Integrated Neutron and Gamma Ray Contributions to the Nuclear Heating Rates in the Catalyzed DD and DT Reactors* (Excluding the Contribution from Th Fission)

Blanket Component	Zone	Catalyzed D-D Plasma (Na-Th-F-Be Salt)				D-T Plasma (Li-Th-F-Be Salt)			
		Neutron Heating Rate (W per n/s)	Gamma Ray Heating Rate (W per n/s)	Total Heating Rate (W per n/s)	Fractional Heating Rate (%)	Neutron Heating Rate (W per n/s)	Gamma Ray Heating Rate (W per n/s)	Total Heating Rate (W per n/s)	Fractional Heating Rate (%)
First Wall	3	4.71×10^{-14}	1.25×10^{-13}	1.72×10^{-13}	14.0	8.64×10^{-14}	1.53×10^{-13}	2.39×10^{-13}	12.8
Water	4	7.39×10^{-14}	7.41×10^{-15}	8.13×10^{-14}	6.6	8.90×10^{-14}	9.26×10^{-15}	9.83×10^{-14}	5.2
Structure	5	3.53×10^{-14}	1.06×10^{-13}	1.41×10^{-13}	11.4	6.46×10^{-14}	1.22×10^{-13}	1.87×10^{-13}	10.0
Molten Salt	6	2.44×10^{-13}	5.86×10^{-13}	8.30×10^{-13}	67.4	7.29×10^{-13}	6.09×10^{-13}	1.34×10^{-12}	71.6
Structure	7	3.75×10^{-16}	4.40×10^{-15}	4.78×10^{-15}	0.4	5.75×10^{-16}	4.03×10^{-15}	4.61×10^{-15}	0.2
Graphite	8	5.70×10^{-16}	1.04×10^{-15}	1.61×10^{-15}	0.1	8.44×10^{-16}	1.09×10^{-15}	1.93×10^{-15}	0.1
Structure	9	5.60×10^{-18}	1.44×10^{-15}	1.44×10^{-15}	0.1	8.67×10^{-18}	1.71×10^{-15}	1.72×10^{-15}	0.1
Total Heating Rate		4.01×10^{-13}	8.31×10^{-13}	1.23×10^{-12}		9.70×10^{-13}	9.00×10^{-13}	1.87×10^{-12}	
MeV Per Source Neutron		2.50	5.19	7.69		6.05	5.62	11.67	
BEMR**		0.30	0.63	0.93		0.43	0.40	0.83	

* Molten salt thickness = 42 cm
 Reflector thickness = 40 cm
 No structure in salt region

** BEMR = Blanket Energy Multiplication Ratio = $\frac{\text{Energy Deposited in the Blanket Excluding Th Fission (MeV)}}{\text{Source Neutron Energy (MeV)}}$

catalyzed DD and DT reactor systems. The energy deposition rates do not include those from the fission of Th in the blanket. In both reactors, $\sim 30\%$ of the plasma neutron and secondary gamma ray energy is deposited in the first structural wall, water cooling channel, and the structural wall that contains the molten salt and $\sim 70\%$ of the energy is deposited in the molten salt compartment. The energy deposition rates in the remaining and the graphite reflector are less than 1% of the total energy deposition rate. The energy deposition rate in the first wall, coolant, and the structure in front of the molten salt is somewhat higher than that calculated in similar components in other fusion reactor designs.²⁹ This is due, in part, to the thickness of the components selected for this study. No effort was made to optimize the thickness of these components since the first wall and coolant dimensions depend on other considerations (e.g., thermodynamic and mechanical).

Also given in Table VIII is the energy deposition in MeV per source neutron and the blanket energy multiplication ratio, BEMR, which is defined as the neutron and gamma ray energy deposited in the blanket in MeV divided by the source neutron energy in MeV. The values do not include the energy deposited from the fission of thorium. The energy production per source neutron is higher in the DT reactor blanket (11.67) than in the DD reactor blanket (7.68). The energy deposited by secondary gamma rays is comparable in both systems while the energy deposited by the plasma neutrons is ~ 2.5 times larger in the DT system than in the DD system. In the DT system, neutrons react with ${}^6\text{Li}$ in the salt with the release of 4.78 MeV per reaction. The blanket energy multiplication ratio is larger in the DD reactor (0.93) than in the DT system (0.83).

A comparison of the energy deposition rates, the Th(n,f) rates, and the blanket energy multiplication ratios in the two salt compositions is shown in Table IX as a function of the plasma neutron source. The total energy deposition rate increases with increasing neutron energy in both salts. The energy deposition rate is largest for both salts for the DT plasma and exceeds that for the 2.45-MeV neutron source by a factor of ~ 2.2 . The total energy deposition rate for the case with the catalyzed DD plasma is just the average of the energy deposition rate for the 2.45 MeV and DT neutron sources. Two values of the blanket energy multiplication are given in the Table. BEMR represents the blanket multiplication ratio excluding the contribution to the multiplication by the energy of fission. When the contribution from the Th fission is included³⁰, the total blanket energy multiplication is given by the value BEMRF which is defined as

$$\text{BEMRF} = \text{BEMR} + \frac{\text{Th}(n,f) \times 184.2 \text{ MeV/fission}}{\text{Source Neutron Energy (MeV)}} .$$

The largest values of BEMRF occur when the plasma is comprised of 2.45-MeV neutrons. However, from the point of view of this study, it is observed that the blanket energy multiplication in the Na salt used in conjunction with the catalyzed DD plasma is larger than that attained in the Li salt used with a DT neutron source by about 7%. The DD system yields a higher fissile fuel breeding rate than the DT system and a higher blanket energy multiplication ratio as well. The energy production per source neutron is, however, higher in the DT system than in the DD system.

The energy deposition rates and the blanket energy multiplication rates for the catalyzed DD and DT systems are compared in Table X as a function of the volume fraction of stainless steel in the molten salt

Table IX. COMPARISON OF THE ENERGY DEPOSITION RATES AND BLANKET MULTIPLICATION RATIOS AS A FUNCTION OF THE PLASMA NEUTRON SOURCE*

Neutron Source	Neutron Heating Rate	Gamma Ray Heating Rate	Total Heating Rate	Th(n,f)	BEMR**	BEMRF**	Total Energy [†] Deposition
	(W per n/s)			Reactions n/s			
	<u>Na-Th-F-Be Salt</u>						
2.45 MeV	1.82×10^{-13}	5.42×10^{-13}	7.24×10^{-13}	7.60×10^{-3}	1.84	2.41	5.90
D-T	6.20×10^{-13}	1.12×10^{-12}	1.74×10^{-12}	3.28×10^{-2}	0.77	1.20	16.90
Cat-D-D	4.01×10^{-13}	8.31×10^{-13}	1.23×10^{-12}	2.02×10^{-2}	0.93	1.38	11.40
	<u>Li-Th-F-Be Salt</u>						
2.45 MeV	4.42×10^{-13}	4.12×10^{-13}	8.54×10^{-13}	9.80×10^{-3}	2.18	2.92	7.15
D-T	9.70×10^{-13}	9.00×10^{-13}	1.87×10^{-12}	3.52×10^{-2}	0.83	1.29	18.14
Cat-D-D	7.06×10^{-13}	6.56×10^{-13}	1.36×10^{-12}	2.25×10^{-2}	1.03	1.53	12.64

* Salt compartment thickness = 42 cm
 Reflector thickness = 40 cm
 No SS-316 in salt

** BEMR = Energy Deposited in the Blanket Excluding Fission (MeV)/Source Neutron Energy (MeV)
 BEMRF = BEMR + Th(n,f) · 184.2 MeV/Source Neutron Energy (MeV)

† MeV/Source Neutron

Table X. Comparison of the Energy Deposition Rates and Blanket Multiplication Ratios in the Catalyzed DD and DT Reactors as a Function of the Volume Fraction of SS-316 in the Molten Salt Compartment*

Fraction of SS-316 in Salt	Neutron Heating Rate	Gamma Ray Heating Rate	Total Heating Rate	BEMR **
(%)	(W per n/s)			
<u>Catalyzed D-D System (Na-Th-F-Be Salt)</u>				
0	4.01×10^{-13}	8.31×10^{-13}	1.23×10^{-12}	0.93
5	3.99×10^{-13}	9.07×10^{-13}	1.31×10^{-12}	0.99
10	3.97×10^{-13}	9.79×10^{-13}	1.39×10^{-12}	1.04
15	3.97×10^{-13}	1.04×10^{-12}	1.44×10^{-12}	1.09
<u>D-T System (Li-Th-F-Be Salt)</u>				
0	9.70×10^{-13}	9.00×10^{-13}	1.87×10^{-12}	0.83
5	9.65×10^{-13}	9.82×10^{-13}	1.95×10^{-12}	0.86
10	9.44×10^{-13}	1.09×10^{-12}	2.03×10^{-12}	0.90
15	9.31×10^{-13}	1.18×10^{-12}	2.11×10^{-12}	0.94

* Salt compartment thickness = 52 cm
 Reflector thickness = 40 cm
 No SS-316 in salt

** BEMR = Total Energy Deposition Excluding Th Fission (MeV)/Source Neutron Energy (MeV)

compartment. For both systems, the neutron energy deposition rate decreases systematically with the addition of stainless steel while the contribution from gamma radiation increases. The total energy deposition rate also increases. The catalyzed DD system gives rise to slightly larger blanket multiplication ratios as the stainless steel is added to the molten salt compartment.

D. Radiation Damage

The atomic displacement rates in the SS-316 blanket structural members are compared as a function of the plasma neutron sources in Table XI for the two salt compositions. For both systems, the atomic displacement rate increases with increasing neutron energy at all locations in the reactor.

The hydrogen and helium gas production rates in the two reactors are compared in Table XII as a function of the plasma neutron source. The gas production rates show the same energy dependent behavior as the atomic displacement rates.

IV. Symbiosis with Fission Reactors and Fuel Production

The purpose of a symbiotic system is to provide fissile fuel for converter reactors. The electrical capacity of converter reactors which the fusion-fission reactors described here can sustain are estimated using the following simplified analysis. Direct conversion of charged particles is not considered.

The power P produced in a set of converter reactors is given by the expression

$$P = U \cdot S_n \cdot E_f \cdot \left(\frac{1}{1-C} \right) \quad (1)$$

Table XI. Comparison of the Atomic Displacement Values in the Structure of the Reactors

Location	Zone	Source	Li-Be-Th-F Salt	Na-Be-Th-F Salt
			$\times 10^{16}$ dpa/(year \cdot neutron \cdot cm)*	$\times 10^{16}$ dpa/(year \cdot neutron \cdot cm)
First Structural Wall	3	I [†]	1.478+0	1.306+0
		II	2.575+0	2.565+0
		III	2.027+0	1.936+0
	5	I	1.149+0	1.021+0
		II	2.058+0	2.047+0
		III	1.604+0	1.534+0
Back Structural Wall	7	I	4.288-3	5.170-3
		II	2.667-2	3.293-2
		III	1.548-2	1.905-2
	9	I	3.164-5	3.660-5
		II	3.730-4	4.568-4
		III	2.023-4	2.467-4

* Based on an effective displacement energy of 40 eV.

42 cm salt region
 40 cm reflector
 no structure in salt region

I: 100% 2.45 MeV

II: 100% 14.06 MeV, D-T

III: 50% 2.45 MeV + 50% 14.06 MeV, catalyzed D-D

Table XII. Comparison of the Gas Production Rates in the Structure of the Reactors

Location	Zone	Source	Li-Be-Th-F Salt		Na-Be-Th-F Salt	
			x 10 ²¹ appm/(yr·neutron·cm)*		x 10 ²¹ appm/(yr·neutron·cm)	
			Hydrogen Gas Production	Helium Gas Production	Hydrogen Gas Production	Helium Gas Production
First Structural Wall	3	I [†]	1.036+0	2.189-4	4.940-1	1.728-4
		II	1.142+1	3.235+0	1.134+1	3.217+0
		III	6.228+0	1.618+0	5.917+0	1.609+0
	5	I	6.906-1	2.752-4	3.280-1	1.288-4
		II	8.505+0	2.370+0	8.414+0	2.346+0
		III	4.598+0	1.185+0	4.371+0	1.173+0
Back Structural Wall	7	I	3.710-4	2.994-6	3.273-4	3.707-6
		II	5.827-2	1.408-2	7.134-2	1.719-2
		III	2.932-2	7.041-3	3.583-2	8.595-3
	9	I	5.077-7	2.522-8	8.000-7	3.063-8
		II	8.258-4	1.701-4	1.032-3	2.165-4
		III	4.132-4	8.506-5	5.164-4	1.083-4

* Atomic parts per million per year per source neutron per cm length (cylindrical geometry)

42 cm salt region
 40 cm reflector
 no structure in salt region

[†]I: 100% 2.45 MeV
 II: 100% 14.06 MeV, D-T
 III: 50% 2.45 MeV + 50% 14.06 MeV, catalyzed D-D

where

- U = fissile nuclei yield per source neutron,
- S_n = neutron source strength,
- E_f = energy released per fission (190 MeV for ^{233}U),
- C = conversion ratio (0.6 for an LWR, 0 for the once-through cycle).

For a 1000 MW(e) two-unit system of 500 MW(e) each³, the total blanket thermal power at 0.33 overall plant efficiency is 3000 MW(th). As indicated in Table IX, the total blanket heating rate for the catalyzed DD reactor is 11.4 MeV per source neutron which implies a source strength $S_n(\text{DD})$ of

$$S_n(\text{DD}) = 3 \times 10^9 \text{ W} \times \frac{1.0}{11.4 \frac{\text{MeV}}{\text{n}} \times 1.602 \times 10^{-13} \frac{\text{J}}{\text{MeV}}} = 1.64 \times 10^{21} \text{ n/s.}$$

For the DT reactor of the same power, the total blanket heating rate is 18.14 MeV per source neutron, so

$$S_n(\text{DT}) = 3 \times 10^9 \text{ W} \times \frac{1.0}{18.14 \frac{\text{MeV}}{\text{n}} \times 1.602 \times 10^{-13} \frac{\text{J}}{\text{MeV}}} = 1.03 \times 10^{21} \text{ n/s.}$$

Also, the rate of fuel production in the two fusion reactor systems is given by

$$K = U \cdot S_n \cdot \left(\frac{M_f}{N_0} \right) \quad (2)$$

where

- M_f = atomic weight of the generated fissile nuclide (^{233}U),
- N_0 = Avogadro's number.

In Eq. (2), U corresponds to the $\text{Th}(n, \gamma)$ reaction rate (decays and transmutations not considered), so

$$K_{DD} = 1.76 \times 10^4 \text{ kg/y} = 5.87 \text{ kg/(y} \cdot \text{MW(th))}$$

and

$$K_{DT} = 9.26 \times 10^3 \text{ kg/y} = 3.09 \text{ kg/(y} \cdot \text{MW(th))}.$$

The catalyzed DD reactor produces about twice as much fissile fuel per blanket MW(th) as the DT reactor. For comparison, the ^{233}U production rates for oxide, carbide, and metal fueled Liquid Metal Fast Breeder Reactors are 0.077, 0.115, and 0.134 kg/y·MW(th), respectively.³¹ For a laser driven hybrid blanket, Maniscalco, Hansen, and Miller report a value of K_{DT} of 1.9 kg/(y·MW(th)). In their blanket, however, the blanket energy multiplication is ~ 20 which arises from the use of a uranium fast fission zone followed by a thorium breeding zone. For the DT reactor molten salt blanket studied here, the blanket energy multiplication is 1.3. In this paper, the investigation was aimed at a fission fuel factory which maximizes fissile fuel production and minimizes power production in the fusion reactor. The use of a molten salt is ideal for this purpose since the fairly continuous separation of the fissile bred fuel will minimize the ^{233}U fissions in the hybrid reactor and the subsequent power production from these fissions. This cannot be readily achieved in a solid-fuel blanket.

Going back to Eq. (1) and assuming 190 MeV is released from the fission of ^{233}U

$$P_{DD} = 0.880 \frac{\text{nuclides}}{\text{neutron}} \times 1.64 \times 10^{21} \frac{\text{n}}{\text{s}} \times \frac{190 \text{ MeV}}{1-\beta} \times 1.602 \times 10^{-19} \frac{\text{MW} \cdot \text{s}}{\text{MeV}}$$

$$P_{DD} = \frac{4.39 \times 10^4}{1-\beta} \text{ MW(th)}$$

and

$$P_{DT} = 0.737 \frac{\text{nuclides}}{\text{neutron}} \times 1.03 \times 10^{21} \frac{\text{n}}{\text{s}} \times \frac{190 \text{ MeV}}{1-\beta} \times 1.602 \times 10^{-19} \frac{\text{MW} \cdot \text{s}}{\text{MeV}}$$

$$P_{DT} = \frac{2.31 \times 10^4}{1-\beta} \text{ MW(th)}.$$

Assuming once again a plant efficiency of 0.33 (neglecting load factors)

$$P_{DD} = \frac{1.7 \times 10^4}{1-C} \text{ MW(e)}$$

and

$$P_{DT} = \frac{7.7 \times 10^3}{1-C} \text{ MW(e)}$$

A 1000 MW(e) two-unit system³ of catalyzed DD or DT reactors can therefore, supply 14.7 and 7.7 reactors, respectively, when operated in the once-through cycle. If Light Water Reactor converters of the same power are employed, the catalyzed DD and DT reactors can fuel 36 and 19 converters, respectively, when $C = 0.6$, with fuel recycle.

Conclusions

A molten salt catalyzed DD symbiotic system coupled to the existing fission reactor economy or LWR advanced converters, as suggested in this study, appears to be an attractive alternative compared to a DT fusion system. The problems attendant to tritium breeding in the blanket, its storage and containment, can be eliminated with the benefit of a higher $\text{Th}(n,\gamma)$ reaction rate due to the absence of the competing ${}^6\text{Li}(n,\alpha)\text{T}$ reaction. Continuous extraction of ${}^{233}\text{U}$ and its ${}^{233}\text{Pa}$ precursor allows relative freedom from fission product contamination, neutron poisoning, and eliminates power swings from ${}^{233}\text{U}$ fissioning in the blanket. This allows better breeding, simpler heat transfer system design, and easier accessibility of reactor components for maintenance, repair, and replacement. The benefits gained from employment of a simple blanket configuration are commercially attractive. The absence of separate neutron multiplying regions and complicated components for containing separate breeding, cooling, and fuel generating systems, while still maintaining substantial fissile production, appears worthy of more detailed investigation.

References

1. D. Steiner and J. F. Clarke, "The Tokamak: Model T Fusion Reactor," *Science* 199, 1395 (1978).
2. D. Steiner, "Nuclear Fusion: Focus on Tokamak," *IEEE Spectrum*, July 1977.
3. D. Steiner et al., "ORNL Fusion Power Demonstration Study: Interim Report," ORNL/TM-5813, March 1977.
4. D. J. Bender, "Performance Parameters for Fusion-Fission Power Systems," UCRL-80589, Rev. 1, May 1978.
5. A. G. Cook and L. M. Lidsky, "The Feasibility of ^{233}U Breeding in Deuterium-Tritium Fusion Devices," MIT Report, March 1977.
6. H. A. Bethe, "The Fusion Hybrid," *Nuclear News*, May 1978.
7. C. W. Gordon and A. A. Harms, "The Basic Characteristics of an Efficient Fusion Breeder," *Atomkerneergie (ATKE)*, Bd. 29 Lfg. 3, 1977.
8. G. La Vergne, J. E. Robinson and J. G. Martel, "On the Matching of Fusion Breeders to Heavy-Water Reactors," *Nuclear Technology* 26, May 1975.
9. A. G. Cook and J. A. Maniscalco, "Uranium-233 Breeding and Neutron Multiplying Blankets for Fusion Reactors," *Nuclear Technology* 30, July 1976.
10. R. W. Conn, S. I. Abdel-Khalik, G. A. Moses and M. Youssef, "The SOLASE-H Laser Fusion Hybrid," *Trans. Am. Nucl. Soc.* 30, 58 (1978).
11. W. E. Parkins, "Engineering Limitations of Fusion Power Plants," *Science*, 199 March 1978.

References (Cont'd)

12. J. P. Holdren, "Fusion Energy in Context: Its Fitness for the Long Term," *Science* 200, April 1978.
13. D. Steiner, "The Nuclear Performance of Vanadium as a Structural Material in Fusion Reactor Blankets," *Nuclear Fusion* 14, (1974).
14. W. R. Grimes and S. Cantor, "Molten Salts as Blanket Fluids in Controlled Fusion Reactors," *The Chemistry of Fusion Technology*, D. M. Gruen, Ed., Plenum Press, NY.
15. H. Nakashima, M. Ohta and Y. Seki, "Nuclear Characteristics of D-D Fusion Reactor Blankets, Survey Calculation, (I)," *J. Nucl. Sci. and Tech.* 14, No. 2, 75 (1977).
16. S. S. Rozhkov and G. E. Shatalov, "Thorium in the Blanket of a Hybrid Thermonuclear Reactor," *US-USSR Symposium on Fusion-Fission Reactors*, July 13-16, CONF-760733, 143, 1976.
17. M. M. H. Ragheb and C. W. Maynard, "Monte Carlo Statistical Weighting Methods for External-Source-Driven Multiplying Systems," UWFDM-265, Fusion Research Program, University of Wisconsin, 1978.
18. M. M. H. Ragheb, M. Z. Youssef, S. I. Abdel-Khalik and C. W. Maynard, "Three-Dimensional Lattice Calculations for a Laser-Fusion Fissile Enrichment Fuel Factory," *Trans. Am. Nucl. Soc.* 30, 59 (1978).
19. V. L. Blinkin and V. M. Novikov, "Symbiotic System of a Fusion and a Fission Reactor with Very Simple Fuel Reprocessing," *Nuclear Fusion* 18, 7 (1978).
20. V. L. Blinkin and V. M. Novikov, "Optimal Symbiotic Molten Salt Fission-Fusion System," IAE-2819, Kurchatov Institute of Atomic Energy, 1977.

21. R. G. Mills, "Catalyzed Deuterium Fusion Reactors," PPL-TM-259, April 1971.
22. D. Steiner, "Neutron Irradiation Effects and Tritium Inventories Associated with Alternate Fuel Cycles for Fusion Reactors," Nuclear Fusion 11, 1971.
23. W. W. Engle, Jr. "A User's Manual for ANISN, A One-Dimensional Discrete Ordinates Code with Anisotropic Scattering," K-1693, Oak Ridge National Laboratory, 1967.
24. W. E. Ford, III, R. T. Santoro, R. W. Roussin and D. M. Plaster, "Modification Number One to the Coupled 100n-21 γ Cross-Section Library for EPR Calculations," ORNL/TM-5249, Oak Ridge National Laboratory (1976).
25. M. A. Abdou, C. W. Maynard and R. Q. Wright, "MACK-A Computer Program to Calculate Neutron Energy Release Parameters (Fluence-to-Kerma Factors) and Multigroup Neutron Reaction Cross Sections from Nuclear Data in ENDF Format," ORNL/TM-3994, Oak Ridge National Laboratory (1973).
26. M. A. Abdou and R. W. Roussin, "MACKLIB 100-Group Neutron Fluence-to-Kerma Factors and Reaction Cross Sections Generated by the MACK Computer Program from Data in ENDF Format," ORNL/TM-3995, Oak Ridge National Laboratory (1974).
27. N. M. Greene et al., "AMPX: A Modular Code System for Generating Coupled Multigroup Neutron-Gamma Libraries from ENDF/B," ORNL/TM-3706, Oak Ridge National Laboratory (1976).

28. T. A. Gabriel, J. D. Amburgey and N. M. Greene, "Radiation-Damage Calculations: Primary Knock-On Atom Spectra, Displacement Rates, and Gas Production Rates," Nucl. Sci. Eng. 61, 21 (1976).
29. R. T. Santoro, V. C. Baker, and J. M. Barnes, "Neutronics and Photonics Calculations for the Tokamak Experimental Power Reactor," Nucl. Tech. 37, 274 (1978).
30. J. J. Duderstadt and L. J. Hamilton, "Nuclear Reactor Analysis," J. Wiley and Sons, NY, (1976).
31. J. A. Maniscalco, L. F. Hansen and W. O. Allen, "Scoping Studies of ^{233}U Breeding Fusion Fission Hybrid," UCRL-80585 (May 1978).

ORNL/TM-6560
Dist. Category UC-20d
MFE-Fusion Systems

Internal Distribution

- | | | | |
|------|---------------------------|--------|--------------------------------|
| 1. | L. S. Abbott | 21-25. | M. J. Saltmarsh |
| 2. | R. G. Alsmiller, Jr. | 26-35. | R. T. Santoro |
| 3-7. | J. M. Barnes | 36. | D. Steiner |
| 8. | D. E. Bartine | 37. | C. R. Weisbin |
| 9. | L. A. Berry | 38. | A. Zucker |
| 10. | G. T. Chapman | 39. | P. Greebler (Consultant) |
| 11. | G. F. Flanagan | 40. | W. B. Loewenstein (Consultant) |
| 12. | T. A. Gabriel | 41. | R. E. Uhrig (Consultant) |
| 13. | H. Goldstein (Consultant) | 42. | R. Wilson (Consultant) |
| 14. | R. A. Lillie | 43-44. | Central Research Library |
| 15. | F. C. Maienschein | 45. | ORNL Y-12 Technical Library |
| 16. | B. F. Maskewitz | | Document Reference Section |
| 17. | O. B. Morgan | 46-47. | Laboratory Records Department |
| 18. | F. G. Perey | 48. | ORNL Patent Office |
| 19. | M. W. Rosenthal | 49. | Laboratory Records - RC |
| 20. | RSIC | | |

External Distribution

50. J. E. Baublitz, Office of Fusion Energy, U.S. Department of Energy, Washington, D.C. 20545
51. F. Coffman, Office of Fusion Energy, U.S. Department of Energy, Washington, D.C. 20545
52. C. R. Head, Systems and Applications Branch, Office of Fusion Energy, G-234, U.S. Department of Energy, Washington, D.C. 20545
- 53-62. M. M. H. Ragheb, Fusion Technology Program, University of Wisconsin, Madison, WI 53706
63. Office of Assistant Manager, Energy Research and Development, DOE-ORO, Oak Ridge, TN 37830
- 64-214. Given distribution as shown in TID-4500, Magnetic Fusion Energy (Distribution Category UC-20d: Fusion Systems)

